The Palaeobotanist 63(2014): 25–32
0031–0174/2014

Petro–chemistry and diagenesis of sandstones of Patherwa Formation, Son Valley, India

M. SHAMIM KHAN*, A.H.M. AHMAD AND R. AGGRAWAL

Department of Geology, Aligarh Muslim University, Aligarh 202 002, India.
**Corresponding author: shamimgeol@gmail.com*

(Received 31 October, 2013; revised version accepted 18 December, 2013)

ABSTRACT

Khan MS, Ahmad AHM & Aggrawal R 2014. Petro–chemistry and diagenesis of sandstones of Patherwa Formation, Son Valley, India. The Palaeobotanist 63(1): 25–32.

The sandstone of Patherwa Formation, (Semri Group) is constituted by quartz, feldspar, micas, rock fragments and heavy minerals. Abrupt changes in the grain size are recorded and sandstone is grouped as fine–grained (FGS), medium–grained (MGS), coarse–grained (CGS) and very coarse–grained (VCGS). The field and petrographic divisions are equally reflected in their chemistry. CGS shows highest SiO_2 content (mean 86.59 wt%) followed by MGS (mean 80.78 wt%), VCGS (mean 76.51 wt%) and FGS (mean 75.21 wt%). ΣREE content is highest in FGS (180.51 ppm) and lowest in CGS (129.64 ppm). VCGS possesses anomalously high ΣREE values (2070.62 ppm). Range of weathering indices including CIA, CIW, PIA and ICV indicates moderate to strong chemical weathering in the provenance. Large range of variation in weathering indices suggests that physical weathering facilitated chemical weathering, under subtropical humid climate. Mechanical compaction led the rearrangement of grains forming point and long contacts while diagenesis dissolved mobile grains which made sandstone highly quartzose. The progressive compaction getting initiated at the sediment–water interface continued till deep burial in a rapidly subsiding basin. Geochemical provenance modelling suggests production of detritus from a predominately granite–gneissic terrain bearing some mafic rocks. Palaeocurrent data indicates sediment supply from two source terrains, i.e. BGC and Bijawar. Synthesis of petrochemical attributes and diagenesis history, assigns a tectonically active setting where generation of positive relief and its desecration was taking place in quick tandem. The most likely such setting is tectonic uplift due to continental collision.

Key–words—Petro–chemistry, Sandstone, Patherwa Formation, Semri Group, Son Valley, India.

भारत में सोन घाटी के पथेरवा शैलसमूह से प्राप्त बलुआपत्थरों का शैल–रसायन एवं प्रसंघनन

एम. शमीम खान, ए.एच.एम. अहमद एवं आर. अग्रवाल

सारांश

पथेरवा शैलसमूह, (सेमरी समूह) का बलुआपत्थर क्वार्ट्ज़, फेल्सपार, अभ्रक, शैल खंडजों और भारी खनिजों से संघटित है। कण आकार में यकायक परिवर्तन अभिलिखित किए गए हैं तथा बलुआपत्थर उत्तम दानेदार (एफ.जी.एस.), मध्यम दानेदार (एम.जी.एस.), स्थूल दानेदार व अति स्थूल दानेदार (वी.सी.जी.एस.) के रुप में समूहित है। उनके रसायन में क्षेत्र एवं सजातीय शैल प्रभाग समान रूप से प्रतिबिंबित हैं। एम.जी.एस. (माध्य 80.78 भार%), वी.सी.जी.एस.(माध्य 76.51 भार%) एवं एफ.जी.एस. (माध्य 75.21 भार%) के अनुगामी सी.जी.एस. अधिकतम SiO_2 अंतर्वस्तु (माध्य 86.59 भार%) दर्शाता है। ∑REE अंतर्वस्तु एफ.जी.एस. (180.51 ppm) में अधिकतम एवं सी.जी.एस.(129.64 ppm) में निम्नतम है। वी.सी.जी.एस. में विषम रूप से उच्च ∑REE मान (2070.62 ppm) है। सी.आई.ए., सी. आई.डब्ल्यु., पी.आई.ए., आइ.सी.वी. सहित अपक्षय अक्षांकों के परिसर प्राप्ति स्थल में मध्यम से उच्च रासायनिक अपक्षय इंगित करते हैं। अपक्षय अक्षांकों में परिवर्तन के विशाल परिसर सुझाते हैं कि उप–उष्णकटिबंधीय आर्द्र जलवायु में रासायनिक अपक्षय भौतिक अपक्षय सुगम हुआ। बिंदु एवं दीर्घ संपर्क गठित करते हुए यांत्रिक संहनन ने दानों की पुनर्व्यवस्था की जबकि प्रसंघनन में चल दाने विलुप्त हो गए जिसने बलुआपत्थर को अति–स्फटिकमय बना दिया। अवसाद–जल अंतरापृष्ठ में शुरू हो रहा प्रगामी संहनन द्रुत रूप से धंसती द्रोणी में अथाह दफन तक चलता रहा। भू–रासायनिक प्राप्ति स्थल प्रतिरूपण पूर्व प्रभावी ग्रेनाइट–नाइसी भू–भाग दिक्मान कुछ मेफिक शैलों से मलबे का उत्पादन सुझाते हैं। पुराधारा आंकड़ा दो स्रोत भू–भागों अर्थात बी.जी.सी. एवं बिजावर से अवसाद पूर्ति इंगित करता है। शैल–रसायन गुण एवं प्रसंघनन इतिहास का संश्लेषण विवर्तनिक रूप से सक्रिय विन्यास नियत करता है जहां सकारात्मक भू–आकृति का जनन एवं इसका दूषण तीव्र अनुबद्ध में हो रहा था। इस तरह का विन्यास ज्यादातर माद्वीपीय संघट्ट की वजह विवर्तनिक उत्थान है।

सूचक शब्द—शैल–रसायन, बलुआपत्थर, पथेरवा शैलसमूह, सेमरी शैलसमूह, सोन घाटी, भारत।

INTRODUCTION

THE Vindhyan Basin of central India is one of the largest and best preserved Proterozoic sedimentary basins of the world, covering a vast area of 1,78,000 km^2. This basin parabolically encloses Archaean domain of Bundelkhand massif and lies in front of Aravalli and Satpura orogenic belts. The margins of the basin are demarcated by an arcuate thrust belt comprising Mesoproterozoic Aravalli–Delhi Fold Belt and the Satpura fold belts (Radhakrishna & Naqvi, 1986). It is believed that the basin was formed as a consequence of the collision of the Bundelkhand Craton with the Deccan Protocontinent in the south and Aravalli Craton in the north during the early Mesoproterozoic Period (Yadekar *et al*., 1990; Raza *et al*., 1993, 2009). Litho sequence of Vindhyan Basin referred to as the Vindhyan Supergroup preserves the thickest Precambrian sedimentary succession in India. The Vindhyan strata are exposed at two major localities: Son Valley and Aravalli–Bundelkhand Craton. Substantially thick Vindhyan rocks have also been recognised under the Gangetic alluvium. The Vindhyan Supergroup has been divided into two groups, viz. Semri Group (Lower Vindhyan) and Kaimur Group (Upper Vindhyan) (Banerjee & Sinha, 1981; Prasad, 1984). Gupta *et al*. (2003) classified Semri Group into eight formations (Table 1). The Semri Group depicts a cyclic sedimentation of rudaceous–arenaceous–argillaceous–carbonate sediments. Three major sedimentation periods, each culminating in a tectono–magmatic activity has been identified in the Semri Group (Gupta *et al.*, 2003). Vindhyan sediments are considered to have deposited in diverse environments ranging from fluvial to deep marine (Bhattacharya & Morad, 1993; Bose & Chakraborty, 1994; Chakraborty, 1993; Chakraborty & Bhattacharya, 1996) to storm dominated sedimentation (Bose *et al*., 1988).

GEOLOGICAL SETUP

In the Son Valley section, the Vindhyan Supergroup unconformably overlies ~ 2500 Ma metamorphites of Bijawar Group (Crawford & Compston, 1970). The Vindhyan Supergroup is bordered by the Aravalli–Delhi orogenic belt (2500–900 Ma, Roy, 1988) in the west and the Satpura orogenic belt (1600–850 Ma, Verma, 1991) to the south and east. The Bundelkhand Massif (3.3–2.5 Ga, Crawford & Compston, 1970; Mondal *et al*., 2002) occurs at the centre of Vindhyan Basin and divides it into two sub–basins–Son Valley in the east and Aravalli's Vindhyan in the west.

Much of the northern part of the Vindhyan Basin along with the Aravalli–Delhi fold belt and the Bundelkhand Massif is overlain by recent alluvium of the Gangetic Plain while the

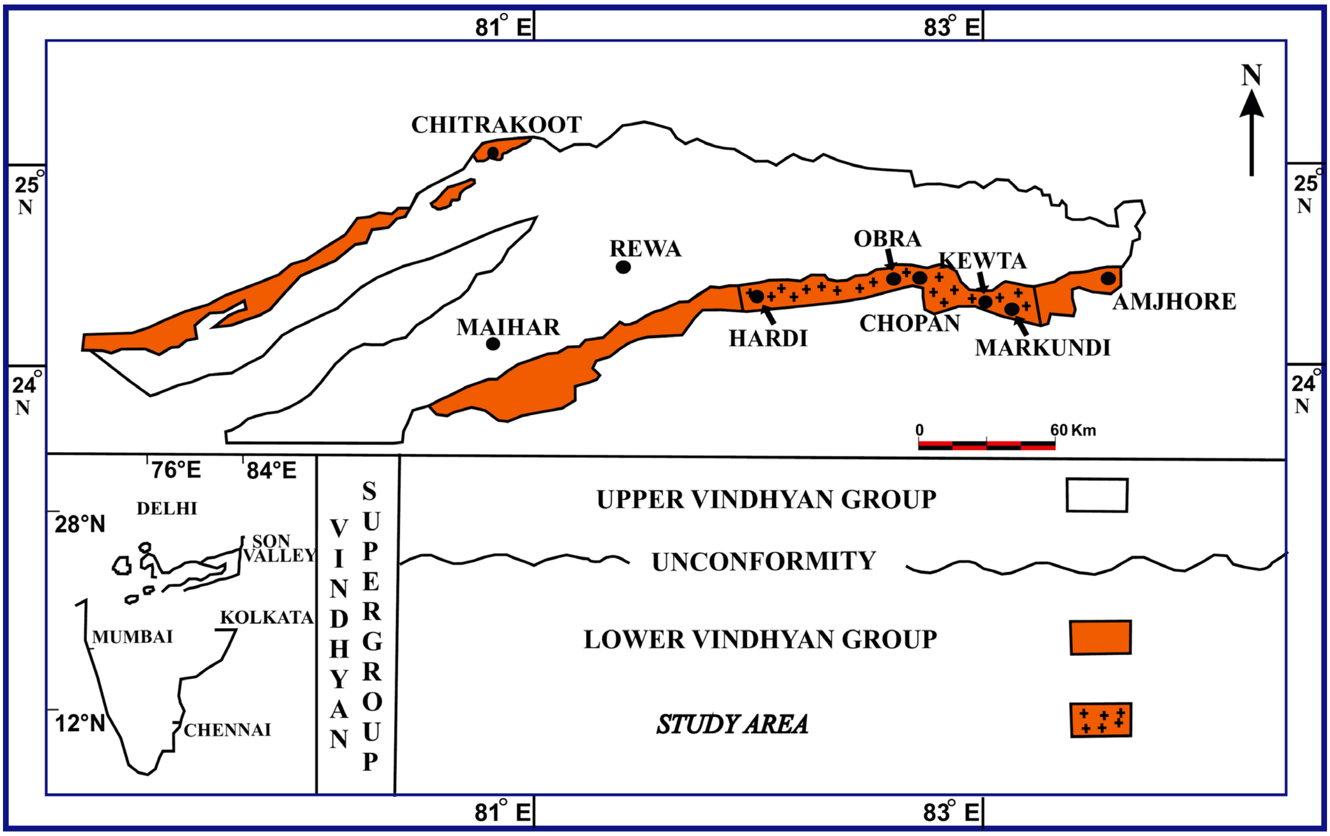

Fig. 1—Geological map of the study area.

Super Group	Group	Formation	Lithology
V I N D H Y A N S U P E R G R O U P	K a i m u r G r o u p	Dhandraul Sandstone	Milky white, compact medium– to fine–grained sandstone & orthoquartzite.
		Scarp Sandstone	Red, pink, compact, blocky sandstone. Khaki & greenish grey; micaceous siltstone and sandstone.
		Bijaigarh Shale	Grey micaceous siltstone, red & yellow olive shale & siltstone black carbonaceous shale & ferruginous sandstone.
		Markundi Sandstone with Susnai breccia at the base	Light greyish white, medium– to fine–grained micaceous sandstone and breccia conglomerate with angular to sub–angular clasts at base.
		Ghurma Shale	Micaceous, yellow, brown and light grey porcelainic shale with interbeds of black carbonaceous shale and siltstone.
		Ghaghar Sandstone	Coarse– to medium–grained pinkish sandstone
		....	.... DISCONFORMITY ....
	S e m r i G r o u p	Rohtas Limestone	Flaggy limestone with cherty parting Black paper–thin shale, porcelainic shale with calcareous nodules. Blocky, massive, light grey, brown, fawn coloured stylolitic limestone interbeds.
		Basuhari Sandstone	Greenish grey, khaki green, olive green and porcelainic shales with siltstone interbeds. Glauconitic sandstone, silty sandstone, greenish grey and khaki to brown quartz arenites.
		Bargawan Limestones	Fawn coloured limestone with quartz veins and black chert bands. Fawn to light grey coloured compact cherty limestone with stromatolites bands. Argillaceous flaggy limestone with siltstone interbeds.
		Kheinjua Shale	Olive to greenish grey khaki splintery shale with calcareous inter–beds and partings.
		Chopan Porcellanite	Light grey, greenish porcelainic shales, ash, tuff, conglomerate beds with arkosic sandstone.
		Kajrahat Limestone	Siliceous, cherty, dolomitic, limestone with stromatolites. Blocky and slabby limestone and dolarenite with argillite interbeds.
		Arangi Shale	Light grey, black, slabby limestone, stylolite bleached, purplish porcelainic shales and black carbonaceous shales.
		Patherwa Sandstone	Gritty to pebbly sandstones, medium–grained sandstone and siltstone. Conglomerate with cobbles, pebbles and clasts of quartz, quartzite, chert, yellow and red jasper set in a sandy matrix.

Sidhi Phyllite   Bundelkhand Granitoid Complex   Mahakoshal Group

Table 1—Stratigraphic succession with litho assemblage of the Vindhyan Supergroup in parts of south Uttar Pradesh (after Das & Jain, 1997; Gupta *et al.*, 2003) around Chopan.

southern part of the basin is covered by Deccan lava Traps. The southern edge of Vindhyan Basin and eastern edge of Bundelkhand Massif are occupied by volcano–sedimentary sequences referred to as Mahakoshal Group (2400 Ma) and the Bijawar Group (2100 Ma) respectively (Krishnan, 1968; Das *et al.*, 1990; Roy & Bandyopadhyay, 1990). The southern edge of the Vindhyan Basin is also marked by a major structural feature called the Narmada–Son lineament which is considered to have formed along Archaean structural trends and remained active throughout the geologic history upto the present (Naqvi & Rodgers, 1987; Kaila *et al*., 1989). South of this lineament, a southerly dipping reverse fault separates the Vindhyan Supergroup rocks from the Satpura belt in the Son Valley (Tewari, 1968). This faulting caused deformation of the Vindhyan sedimentary rocks exposed immediately to the north but can not be traced further west, as it is possibly covered by the Great Boundary Fault, another major lineament characterised by westerly dipping faults, which separates the Vindhyan from the Aravalli–Delhi fold belt rocks. Major part of the basin consists of unmetamorphosed sediments providing suitable environments for the deposition of hydrocarbons. The present study mainly aims at reconstructing the sedimentation and diagenetic history of the Patherwa Formation (Semri Group) in eastern Vindhyan Basin (Fig. 1).

METHODOLOGY

Lithostratigraphic sections were studied from well exposed outcrops at various locations along the strike of the study area (Fig. 1). Samples were collected from various locations and different horizons in and around the area. Detrital mineralogy of the sandstones was studied for the purpose of description and interpretation of their provenance. An attempt was made to study the diagenetic history of the sediments. Ninety three thin sections were analysed to study the types of grain contacts, porosity reduction and cementation. Thirty one samples were analysed for their major element by XRF at NIO, Goa using bead pellets and trace elements including REEs were analysed by ICP–MS at NGRI, Hyderabad.

LITHOFACIES AND DEPOSITIONAL ENVIRONMENT

Sandstone of Patherwa Formation display variations in grain size and structures in vertical disposition. Main variations are exemplified by conglomeratic, pebbly and thinly bedded varieties. In terms of structures, trough and herringbone cross–beds and ripples are very well preserved in the sandstone. Synthesis of the grain size and structures assigns three genetically related depositional environments, viz. (i) Tidally influenced fluvial channel, (ii) Tidal channel and (iii) Tidal sand bar / tidal sandy flat for the deposition of Patherwa Formation.

DETRITAL MINERALOGY

The Patherwa Formation Sandstone chiefly consists of quartz (~ 92 vol. %). This quartz mode comprises common quartz (96 vol. %) and recrystallised metamorphic quartz (6 vol. %). Feldspars are present in fresh and altered forms. Alteration and leaching of the feldspar grains is observed along cleavage planes and grain boundaries. Rock fragment observed in these sandstone include chert, shale, schist, phyllite, quartzite and tuff. Both muscovite and biotite occur as

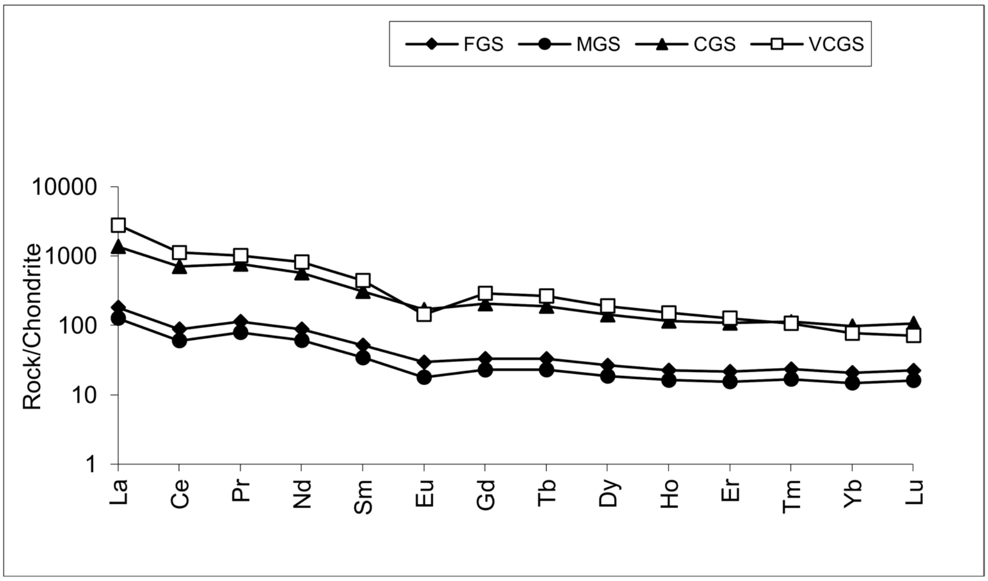

Fig. 2—Chondrite normalised average REE profiles of Patherwa Formation sandstone (FGS=Fine–Grained Sandstone, MGS=Medium–Grained Sandstone, CGS=Coarse–Grained Sandstone, VCGS=Very Coarse–Grained Sandstone). Normalising values from Sun and McDonough (1989).

	CQ	RMQ	SMQ	Mica	Chert	Plagioclase	Microcline	RF
	Hardi Section							
Range	76–96	0–6	0–8	0–12	0–1	0–7	0–8	0–2
Average	86	3	2	3	1	2	2	1
	Obra Section							
Range	61–89	0–19	0–10	0–14	0–2	0–6	0–6	0–4
Average	79	6	4	5	1	2	2	1
	Kewta Section							
Range	79–96	0–7	1–10	0–4	0–3	0–3	0–3	0–3
Average	88	2	4	2	1	1	1	1
	Markundi Section							
Range	74–92	0–11	0–8	0–8	0–2	0–4	0–5	0–4
Average	85	5	2	1	1	2	2	2

Table 2—Range and average of detrital models of Patherwa Formation Sandstone, Son Valley, India (CQ = Common Quartz, RMQ = Recrystallised Metamorphic Quartz, SMQ = Stretched Metamorphic Quartz, RF = Rock Fragments).

tiny to large elongate flakes with frayed ends. Heavy minerals include opaque, tourmaline, zircon, biotite, epidote, garnet, staurolite, hornblende and rutile (Tiwari & Yadav, 1993; Table 2). The Vindhyan Basin covers a large part of the northern Indian shield and rests on a wide variety of basement rocks including the Banded Gneissic Complex in the northern part and the Bijawar Group, the Chotanagpur Granite–Gneiss (CGG) and the Mahakoshal Group in central and western part of India. The palaeocurrent directions for the Vindhyan sediments are mostly northerly and northwesterly (Bose *et al*., 2001). It suggests supply of detritus into Vindhyan Basin from Chotanagpur Granite – Gneiss terrain and Bijawar Group (granite, granodiorite, pegmatite, gneiss and mafic volcanics) also in addition to Banded Gneissic Complex of Aravalli Craton.

GEOCHEMISTRY

On the basis of grain size, sandstones under study are divided into four groups, viz. Fine Grain Sandstone (FGS), Medium Grain Sandstone (MGS), Coarse Grain Sandstone (CGS) and very Coarse Grain Sandstone (VCGS). These groupings of the sandstones are characteristically reflected in their geochemical composition. For example, CGS has highest SiO_2 content (mean 86.59 wt. %) followed by MGS (mean 80.78 wt.%), VCGS (mean 76.51 wt.%) and FGS (mean 75.21 wt.%). The Al_2O_3 content is strongly negatively correlated with SiO_2 in each group and thus their mean Al_2O_3 abundance is reverse to that of mean SiO_2, FGS (10.23 wt.%), VCGS (9.86 wt.%), MGS (4.86 wt.%) and CGS (3.42 wt.%). Mean SiO_2/Al_2O_3 ratio of FGS, MGS, CGS and VCGS is 8.69, 25.65, 45.03 and 7.77 respectively suggesting that FGS and VCGS are texturally immature while MGS and CGS are mature sandstones. The REE profiles of all the samples are similar to those of Proterozoic sediments (Taylor & McLennan, 1985) showing LREE enrichment and significant sink at Eu (Fig. 2). However, there is distinct zonation in terms of average REE abundances as FGS and MGS, and CGS and VCGS varieties possess like abundances. But VCGS bears largest Eu/Eu^* value (0.40) and maximum LREE enrichment. Compared to PAAS (Fig. 3), each variety is depleted in major oxides. FGS and MGS show nearly equal or slightly depleted abundance of LILE and severe depletion in TTE (except Co). CGS is strongly enriched in LILE, REE and TTE. On the other hand VCGS is strongly enriched in REE but possesses similar abundance of TTE like that of FGS and MGS. Furthermore, Zr is high in all varieties compared to PAAS. It suggests that either the conditions of sediment generation or transportation agency and / or its intensity changed which sorted significantly different trace element abundances. The ΣREE abundances bear inverse relation to grain size, i.e. FGS are most enriched in ΣREE where as CGS possess least ΣREE abundance. The ΣREE content of VCGS seems to have been controlled by a heavy mineral phase (other than zircon) as it possesses anomalously high values of ΣREE (1896.71 ppm). It appears that grain size sorting (accumulation of fine fraction) have controlled the ΣREE contents to large extent.

The weathering indices including CIA, CIW, PIA and ICV indicate increasing trend of chemical weathering from FGS to CGS (moderate to strong) (Table 2). It may be suggested that initially it was the physical weathering which dominated sediment production, however, quiescence in tectonic activity paved the way for the enhanced role of chemical weathering under subtropical humid climate in the catchment area. Geochemical provenance modelling suggests derivation of detritus for these rocks from granite–gneiss terrain having significant proportion of mafic rocks either as enclaves (BGC terrain) or flows (Bijawar terrain).

DIAGENETIC EVOLUTION

The grains of sandstone under study shows long contacts (63%), point contacts (15%), concavo–convex contacts (7%), sutured contacts (5%) and floating grains (10%). There are five types of cements namely silica, iron oxide, carbonate, dolomite and glauconite in variable proportions. Petrographic attributes indicate that mechanical compaction was the operative during early stage of diagenesis which caused rotation and adjustment of grains and formation of point and long contacts. Compaction, largely influenced by roundness of detrital particles was possible in the absence of an early major cementation phase that could have stabilised the detrital framework. Chemical dissolution of quartz and formation of silica cement resulted during first stage of burial. Subsequent burial event led to alteration of feldspars and its dissolution. The shallow depth of burial and lack of illitization suggest that the feldspar in the studied sandstones were destroyed in the shallow weathering zone (McBride, 1985).

The sandstones under study show two contrasting diagenetic histories. Lower Group was subjected to more compaction than cementation indicated by low porosity while Upper Group suffered more cementation than compaction and thus possesses high primary porosity. This diagenetic division is equally preserved in their geochemical composition too.

The range and average of weathering indices of all the sandstones assign them low to moderate chemical weathering, while their labile contents show inverse relationship with the grain size without any appreciable change in the concentration of their major oxides. Moreover, their HFSE contents, in particular Zr shows effect of grain size sorting and recycling. All these factors suggest that all the sandstones had low primary porosity due to early cementation followed by compaction. However with increasing depth of burial dissolution of carbonates, iron oxides and feldspar took place. Coarsening of grains acted as a catalyst to the dissolution process. Consequently medium– to coarse–grain sandstone attained secondary porosity where as the dissolved ions got accumulated in fine grain sandstone, there by further reducing its porosity. It is therefore inferred that diagenesis through chemical reaction played active role in enhancing the porosity (secondary) in these sandstones.

CONCLUSIONS

The modal mineralogy and petrographic characters of Patherwa Formation sandstone is attributed to tidal processes. The Chotanagpur Granite–Gneiss (CGG) and Bijawar Group comprising granite–granodiorite, pegmatite–gneiss and

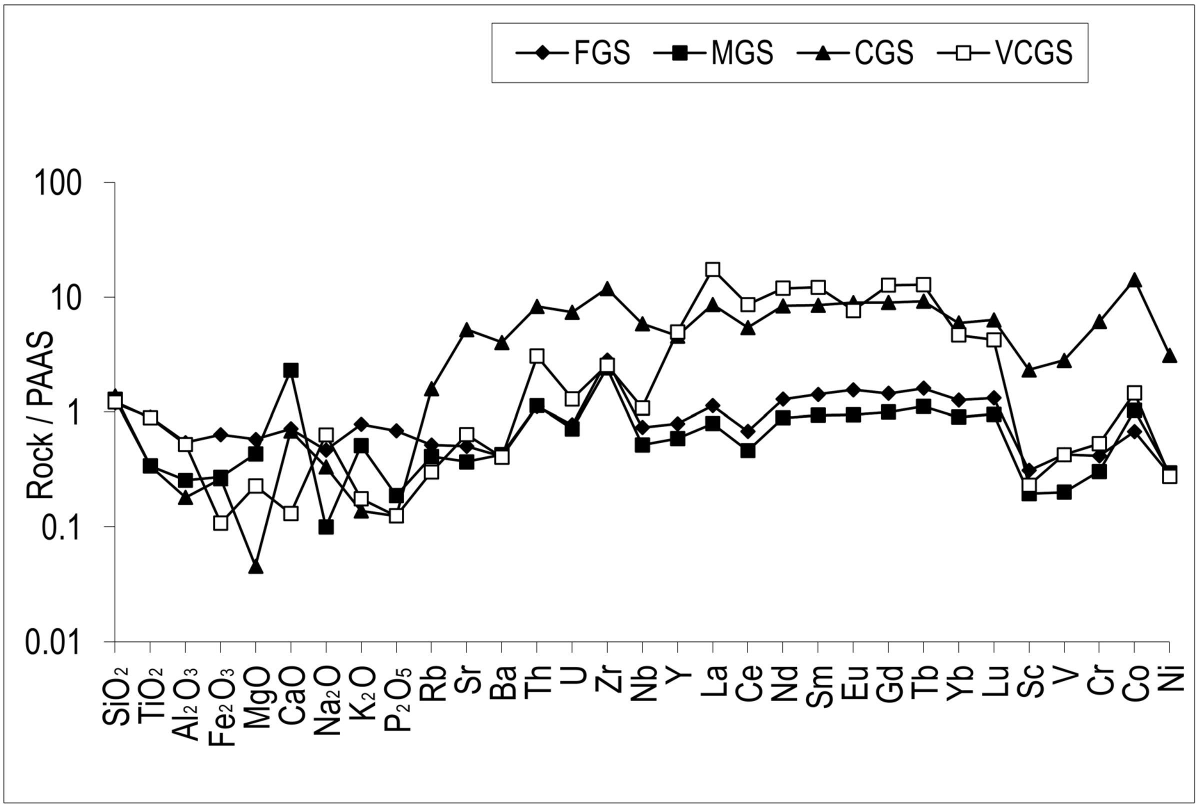

Fig. 3—PAAS normalized multielement spidergram of average abundances of Patherwa Formation sandstone (FGS=Fine–Grained Sandstone, MGS=Medium–Grained Sandstone, CGS=Coarse–Grained Sandstone, VCGS=Very Coarse–Grained Sandstone). Normalising values from Condie (1993).

	F.G.S.		**M.G.S.**		**C.G.S.**		**V.C.G.S.**
Elements	Range	Average	Range	Average	Range	Average	
SiO_2	56.12–82.9	75.21	64.22–93.26	80.78	72.7–95.78	86.59	76.57
Al_2O_3	5.79–24.36	10.23	1.12–10.52	4.80	1.06–9.36	3.42	9.86
TiO_2	0.58–1.37	0.90	0.09–0.93	0.34	0.08 0.73	0.34	0.89
Fe_2O_3	1.49–7.78	4.13	0.38–3.45	1.76	0.36–6.71	1.71	0.70
MnO	0.01–0.07	0.03	0.01–0.1	0.04	0.03–0.04	0.04	0.00
MgO	0.12–3.08	1.27	0.03–5.16	0.95	0.02–0.25	0.10	0.50
CaO	0.15–4.17	0.93	0.03–12.24	2.99	0.03–5.07	0.89	0.17
Na_2O	0.01–0.77	0.56	0.02–0.3	0.12	0.27–0.53	0.40	0.76
K_2O	1.61–3.98	2.90	0.58–2.72	1.89	0.08–1.7	0.51	0.65
P_2O_5	0.04–0.18	0.11	0.01–0.05	0.03	0.01–0.03	0.02	0.02
SiO_2/Al_2O_3	2.37–14.19	8.69	7.23–81.13	25.65	7.77–90.53	45.03	7.77
CIA	63.45–90.5	68.26	54.37–89.93	63.89	62.46–87.18	78.13	81.38
PIA	76.89–96.54	85.92	87–95.71	92.07	73.19–95.14	89.66	85.48
CIW	83.28–96.78	90.63	95.05–98.51	96.99	74.94–96.24	91.24	86.37
ICV	0.29–1.84	1.09	0.25–2.2	1.17	0.52–1.75	1.10	0.37
Sc	2.21–11.5	4.98	1.32–6.13	3.11	0.91–6.03	37.10	3.69
V	29.53–153.48	63.83	8.41–61.92	30.15	10.06–57.95	420.68	63.73
Cr	21.08–77.18	45.76	20.29–63.79	33.42	28.54–71.14	674.38	58.27
Co	10.33–18.63	15.56	9.49–61.77	23.75	5.31–42.53	325.78	33.63
Ni	10.16–19.61	15.76	12.65–19.02	16.24	7.63–18.44	170.98	15.16
Rb	63.55–107.54	82.63	20.97–99.59	65.53	7.43–43.29	254.54	48.05
Sr	28.99–247.94	100.64	28.64–160.97	73.64	38.76–140.32	1041.24	127.38
Y	12.19–44.02	21.32	7.28–27.53	15.89	6.57–11.11	123.42	134.09
Zr	252.89–998.21	593.17	205.34–914.11	506.79	48.11–365.74	2491.64	534.41
Nb	6.51–30.03	13.97	3.08–23.42	9.82	2.05–19.04	111.30	20.60
Ta	0.51–7.94	3.30	3.02–13.1	5.84	0.56–16.23	76.06	10.49
Ba	193.5–373.83	265.06	149.78–517.73	276.74	112.92–293.38	2612.94	262.86
La	25.37–87.1	43.16	11.39–64.46	30.21	12.64–40.33	327.10	662.24
Ce	29.93–110.15	54.33	14.76–64.24	36.97	23.61–43.28	433.96	687.44
Pr	6.26–20.76	10.83	3.09–15.61	7.55	2.66–9.32	72.90	96.29
Nd	23.9–76.22	41.36	11.73–59.03	28.45	9.76–33.5	268.00	382.72
Sm	4.72–14.35	7.94	2.16–11.03	5.25	1.94–5.68	47.52	68.02
Eu	0.95–3.23	1.71	0.43–1.69	1.04	0.54–0.93	9.84	8.40
Gd	4.07–11.79	6.83	1.93–9.58	4.70	1.81–4.5	42.22	59.76
Tb	0.73–2.53	1.24	0.36–1.69	0.86	0.32–0.7	7.10	9.90
Dy	3.89–15.2	6.75	2.14–8.7	4.74	1.84–3.19	36.18	48.55
Ho	0.75–2.96	1.28	0.45–1.57	0.92	0.34–0.56	6.56	8.57
Er	2.09–7.96	3.59	1.22–4.2	2.57	0.92–1.58	17.96	21.06
Tm	0.36–1.34	0.60	0.19–0.67	0.43	0.2–0.26	2.88	2.74
Yb	2.22–7.65	3.55	1.19–3.9	2.53	0.91–1.53	16.70	13.11
Lu	0.36–1.19	0.57	0.18–0.63	0.41	0.14–0.24	2.72	1.82
Hf	6.88–43.73	22.55	8.51–40.25	22.05	1.99–17.42	103.56	26.35
Th	7.37–44.34	16.29	5.45–40.97	16.58	1.85–19.46	121.04	44.67
U	1.27–4.2	2.40	1.31–3.4	2.21	0.84–2.43	22.86	4.02
Th/U	3.4–11.08	6.72	2.05–17.6	7.45	0.76–12.49	75.30	11.10
Eu/Eu*	0.43–0.89	0.73	0.5–0.86	0.68	0.52–0.88	0.78	0.40
∑REE	318.74–108.64	180.51	51.5–246.96	126.60	58.4–145.61	129.64	2070.62

Table 3—Range and average of major (in wt. %) and trace (in ppm) elements of Patherwa Formation Sandstone, Son Valley, India (F.G.S.=Fine–Grained Sandstone, M.G.S.=Medium–Grained Sandstone, C.G.S.=Coarse–Grained Sandstone, V.C.G.S.=Very Coarse–Grained Sandstone).

mafic volcanics also supplied detritus to the Vindhyan Basin apart from the Banded Gneissic Complex for the deposition of Patherwa Formation sandstone. Diagenetic signatures observed in the studied sandstone include different stages of compaction, cementation and porosity. Geochemical parameters suggest that diagenesis played active role in producing porosity (secondary) in these sandstones.

Acknowledgements*—We gratefully acknowledge the help received from the Chairman, Department of Geology, Aligarh Muslim University, Aligarh for providing the laboratory facilities and other logistics in the Department for completion of this work.*

REFERENCES

Banerjee AK & Sinha PN 1981. Structure and tectonics of Vindhyan in eastern Rajasthan: Miscellaneous Publications Geological Survey of India 50: 41–47.

Bhattacharya A & Morad S 1993. Proterozoic braided ephemeral fluvial deposits: An example from the Dhandraul Sandstone Formation of the Kaimur Group, Son Valley, central India. Sedimentary Geology 84: 101–114.

Bose PK & Chakraborty PP 1994. Marine to fluvial transition: Proterozoic Upper Rewa Sandstone, Maihar, India. Sedimentary Geology 89: 285–302.

Bose PK, Ghosh G, Shome S & Bardhan S 1988. Evidence of superimposition of storm waves on tidal currents in rocks from the Tithonian–Neoconian Umia Member, Kutch, India. Sedimentary Geology 54: 321–329.

Bose PK, Sarkar S, Chakrabarty S & Banerjee S 2001 .Overview of the Meso to Neoproterozoic evolution of the Vindhyan Basin, central India. Sedimentary Geology 141: 395–419.

Chakraborty C & Bhattacharya A 1996. The Vindhyan Basin: an overview in the light of current perspectives. Memoirs of Geological Society of India 36: 301–312.

Chakraborty C 1993. Proterozoic Kaimur Group, Son Valley, India. Facies and sequence in tectono–geographic frame with special bearing of clastic sedimentation: Unpublished Ph.D. thesis submitted to Jadavpur University, Calcutta.

Condie KC 1993. Chemical composition and evolution of the upper continental crust: Contrasting results from surface samples and shales. Chemical Geology 104: 1–37.

Crawford AR & Compston W 1970. The age of the Vindhyan system of peninsular India. Quaternary Journal of Geological Society of London 125: 351–371.

Das LK, Mishra DC, Ghosh D & Banerjee B 1990. Geomorphic tectonics of the basement in a part of Upper Son Valley of the Vindhyan Basin. Journal of Geological Society of London 125: 351–371.

Das S & Jain KC 1997. Final report on the specialized thematic mapping of Vindhyan Supergroup, south U.P., Unpublished GSI Report (F.S.1990–91, to 1994–95).

Gupta S, Jain KC, Srivastava VC & Mehrotra RD 2003. Depositional environment and tectonism during the sedimentation of the Semri and Kaimur groups of rocks, Vindhyan Basin. Journal of Palaeontological Society of India 48: 181–190.

Kaila KL, Murthy PPK & Hall DM 1989. The evolution of Vindhyan Basin vis–à–vis the Narmada–Son Lineament, central India, from deep seismic soundings. Tectonophysics 162: 277–289.

Krishnan MS 1968. Geology of the India and Burma. Higginbothams Ltd. Madras, 5th Edition: 1–536.

McBride EF 1985. Diagenetic processes that effects provenance determination in sandstone. *In*: G.G. Zuffa (Editor)—Provenance of Arenites. Reidel, Dordrecht–Boston–Lancaster: 95–114.

Mondal MEA, Goswami JN, Deomurari MP & Sharma KK 2002. Ion microprobe $^{207}Pb/^{206}Pb$ ages of zircons from the Bundelkhand Massif, northern India: implications for crustal evolution of the Bundelkhand–Aravalli Protocontinent. Precambrian Research 117: 85–100.

Naqvi SM & Rodgers JJW 1987. Precambrian Geology of India; Oxford Monographs on Geology and Geophysics. 6: 1–223.

Prasad B 1984. Geology, sedimentation and palaeogeography of the Vindhyan Supergroup, SE Rajasthan. Memoirs of Geological Survey of India, Miscellaneous Publication 116: 1–148.

Radhakrishna BP & Naqvi SM 1986. Precambrian continental crust of India and its Evolution. Journal of Geology 94: 145–166.

Raza M, Jafri SG, Alvi SH & Khan MS 1993. Geodynamic evolution of Indian shield during Proterozoic: evidence from mafic volcanic rocks. Journal of Geological Society of India 41: 455–469.

Raza M, Khan A & Khan MS 2009. Origin of late palaeoproterozoic great Vindhyan Basin of north Indian shield: Geochemical evidence from mafic volcanic rocks. Journal of Asian Earth Science 34: 716–730.

Roy AB 1988. Stratigraphic and tectonic framework of the Aravalli Mountain Range. India. Memoirs of Geological Society of India 7: 33–75.

Roy S & Bandyopadhyay BK 1990. Cleavage development in Mahakoshal Group of rocks of Sleemanabad–Siroha area, Jabalpur District. Madhya Pradesh. Indian Minerals 44: 111–128.

Sun SS & McDonough WF 1989. Chemical and isotopic systematics of oceanic basalts: Implications for mantle composition and processes: Geological Society of London Special Publication 42: 313–345.

Taylor SR & McLennan SM 1985. The continental crust: its composition and evolution: an examination of the geochemical record preserved in sedimentary rocks. Blackwell Science, Oxford, 312p.

Tewari AP 1968. A new concept of palaeotectonic setup of a part of northern peninsular India with special reference to the great boundary faults. Geologie en Mijnbouw 47: 21–27.

Tiwari RN & Yadav RNS 1993. Concentration of heavy minerals in Son River. Current Science 65: 881–883.

Verma RK 1991. Geodynamic of the Indian Peninsula and Indian Plate margins. Oxford and IBH. Pp 357.

Yadekar DB, Jain SC, Nair KKK & Dutta KK 1990. The Central Indian Collision Suture. Geological Survey of India, Special Publications 28: 1–43.